RAPID COMMUNICATIONS

PHYSICAL REVIEW A **73**, 041406(R) (2006)

Temporal separation of H_2 double-ionization channels using intense ultrashort 10-fs laser pulses

S. Saugout and C. Cornaggia
CEA Saclay, Direction des Sciences de la Matière, Service des Photons, Atomes et Molécules, Bâtiment 522,
F-91 191 Gif-Sur-Yvette, France

(Received 22 November 2005; published 27 April 2006)

Double ionization channels of H_2 are separated in the time domain using ultrashort 10-fs laser pulses in the $10^{13}-10^{15}$ W cm^{-2} intensity range. Charge resonance enhanced ionization does not contribute anymore to double ionization because the H_2^+ ion does not have enough time to stretch up to the critical internuclear distance. Using a pump-probe excitation scheme, this process is shown to be very sensitive for the detection of pre- and post-pulses situated at a few tens of femtoseconds from the maximum pulse envelope.

DOI: 10.1103/PhysRevA.73.041406 PACS number(s): 33.80.Rv, 33.80.Eh, 42.50.Vk

Molecular hydrogen has been extensively studied using femtosecond intense laser pulses in the $10^{13}-10^{15}$ W cm^{-2} in order to understand the molecular dynamics in ultrashort strong laser fields. Substantial progress has been achieved since the early 1990s and is reported in several review papers [1–3]. Bond softening and charge resonance enhanced ionization of the H_2^+ ion are among typical molecular effects with no counterpart in strong field atomic physics [4,5]. In the meantime, advances in ultrafast laser physics led to the availability of intense pulses as short as 5 fs in the 10^{15} W cm^{-2} laser intensity range [6,7]. The H_2 or D_2 molecules are of great interest as possible diagnostics for these pulses due to the two relevant attosecond and femtosecond time scales for, respectively, the electronic and nuclear motion, and very fast dissociation times due to light H, H^+, D, and D^+ atoms and ions. For instance, in a recent experiment, the vibrational motion of the D_2^+ ion was observed with a space and time precision of, respectively, 0.05 Å and 200 as using the entanglement between the electronic wave packet formed from multiphoton ionization of the neutral D_2 molecule and the vibrational wave packet of the resulting D_2^+ ion [8].

In this Rapid Communication we report the ultrafast highly sensitive ionization pattern of H_2^+ ions as a function of the laser pulse duration and possible pre-pulse and post-pulse wings. Indeed, as soon as H_2^+ is produced via the tunnel ionization of neutral H_2, this molecular ion is instantaneously submitted to the high laser field that strongly mixes the bound electronic ground state $X\,^2\Sigma_g^+$ and the dissociative first excited state $A\,^2\Sigma_u^+$. These states correlate to the same dissociation limit $H(1s)+H^+$ and are strongly radiatively coupled by a charge resonance dipole moment. This coupling leads to the dissociation of the molecular ion via bond softening and dressed molecular states crossings [1–3]. It should be emphasized that in this case, the corresponding fragmentation channel is $H(1s)+H^+$.

While the H_2^+ ion is in the course of dissociation, it may be ionized by the strong laser field. This ionization produces two bare protons following the fast departure of the electron. The resulting repulsion energy $E=e^2/4\pi\epsilon_0 R$ between both protons experimentally allows a straightforward determination of the internuclear distance R prior to the ionization event. The ionization rate of H_2^+ as a function of the internuclear distance presents a large enhancement at internuclear distances in between 2 and 7 Å [5]. This anomalously high ionization of H_2^+ was referred to as charge resonance enhanced ionization by Zuo and Bandrauk because its origin is to be found in the charge resonance coupling the X and A states of H_2^+. This effect demands a substantial molecular stretching since the equilibrium internuclear distances of H_2 and H_2^+ are, respectively, 0.741 and 1.052 Å. In addition, a recent experiment found that the H_2^+ ion is produced in its lowest vibrational levels following ionization of H_2 at 800 and 1064 nm [9]. Taking into account that the outer turning points of the $v^+=0,1,2$ vibrational levels of H_2^+ lie below 1.6 Å, charge resonance enhanced ionization does not occur instantaneously and demands enough time for a significant increase of the internuclear distance. In Refs. [10,11] performed at 800 nm and pulse durations in between 28 and 80 fs, the proton spectra confirm the above described charge resonance enhanced ionization. The H^+ ions with a kinetic energy of 3 eV at the maximum of the ion spectra in Ref. [11] come from the ionization of H_2^+ at the internuclear distance $R=2.4$ Å. On the other side, the ionization of H_2^+ at short internuclear distances R below 2 Å is much less probable because of the increase of the ionization limit $E=e^2/4\pi\epsilon_0 R$ as R decreases. In the following, we will denote this process as short range double ionization in order to include all the mechanisms, leading to two bare protons from the H_2 neutral molecule that are not linked to charge resonance enhanced ionization. In particular, short range double ionization includes ionization paths related to nonsequential double ionization of H_2. These protons created at short internuclear distances are more energetic than the protons from resonance enhanced ionization and appear at much higher laser intensities. Moreover, short range double ionization does not need any molecular stretching and hence sufficiently long pulses. As a consequence, charge resonance enhanced ionization is expected to disappear using ultra-short laser pulses while short range double ionization will give the dominant contribution to the proton signals.

Until now, charge resonance enhanced ionization and short range double ionization were identified and compared using a single pulse excitation with durations longer than ~30 fs and proton spectra analysis. In this Rapid Communication, we show that both processes can be separated using

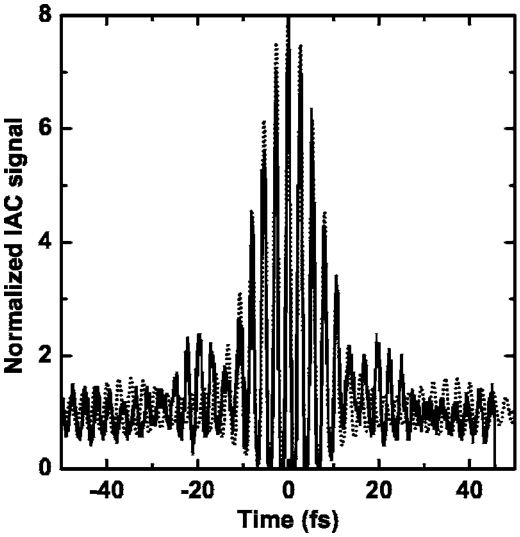

FIG. 1. Interferometric autocorrelation (IAC) of 10-fs laser pulses. The experimental and calculated signals are given, respectively, by the full and dotted curves. The IAC curve is calculated using the Fourier transform of the frequency domain electric field and assuming a constant spectral phase.

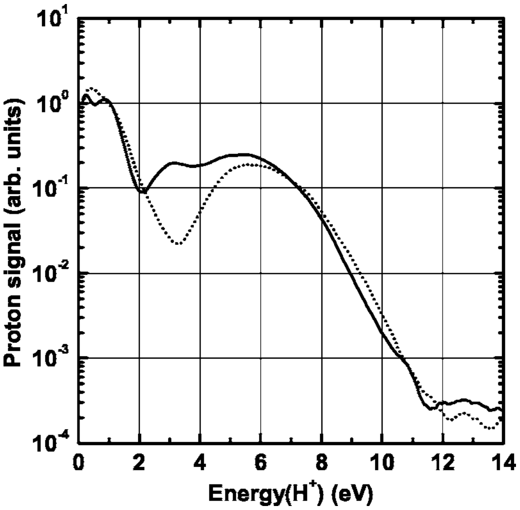

FIG. 2. Proton spectra recorded from H_2 using 10-fs laser pulses at 3.2×10^{15} W cm^{-2} peak intensity. Full curve: no group delay dispersion compensation. Dotted curve: insertion of a 2-mm-thick fused silica plate in the laser optical path for group delay dispersion compensation.

10-fs laser pulses and a time domain analysis based on a pump-probe excitation setup. In particular, charge resonance enhanced ionization is no more observed with 10-fs laser pulses that strongly favor short range double ionization channels. This very fast dynamics might be interesting regarding ultrashort pulses with durations below 10 fs because charge resonance enhanced ionization is shown here to be very sensitive to the presence of pre-pulses or post-pulses around the main pulse.

The 1-kHz Ti:sapphire laser system and pulse compression setup have been described elsewhere [12]. In brief, the pulse compression stage is designed following techniques introduced by Nisoli *et al.* [6] and Sartania *et al.* [7]. The laser spectrum is broadened in a 700-mm-long hollow fiber with a 250-μm inner diameter. The nonlinear Kerr effect takes place in argon at a pressure of 700 mbar for 40-fs and 600-μJ laser input pulses. After recollimation by an $f=1$ m concave silver mirror, pulses are recompressed to 10 fs using several reflections on broadband chirped mirrors. The spectrum and pulse duration are measured using, respectively, a commercial spectrometer and a homemade interferometric autocorrelator. Figure 1 presents an interferometric autocorrelation of 10-fs pulses. The corresponding spectrum exhibits a three-peak structure over around 200 nm due to self-phase modulation in argon gas [12]. The interferometric autocorrelation is calculated, assuming a constant spectral phase. The good agreement between the measured and calculated curves shows that the chirped-mirrors compression stage works well. The remaining disagreement comes from cubic and quartic residual phase that cannot be compensated with our setup. In order to perform pump-probe experiments, ultrashort pulses are sent in a Michelson interferometer with an adjustable delay between both arms. Additional chirped mirrors are used in order to compensate for the group delay dispersion introduced by the beamsplitters. The results presented here were recorded using a single pulse and both pulses from the interferometer. Molecular hydrogen ions and protons are detected using a 1150-mm-long time-of-flight spectrometer based on the Wiley-McLaren configuration and devoted to experimental studies of multiple ionization [13]. Fragmentation channels and the associated kinetic energy release spectra are determined using covariance mapping introduced by Frasinski *et al.* [14].

Group delay dispersion must be compensated when operating the ion spectrometer because of different amounts of optical material in the optical paths on the way to the interferometric autocorrelator and to the ion spectrometer. Figure 2 shows two proton spectra following the single ionization of H_2 and the dissociation of H_2^+ via H^++H for protons with energies below 2 eV and double ionization of H_2 for protons with energies above 2 eV. Double ionization leads to the H^++H^+ dissociation channel, which is identified using covariance mapping. Following the introduction of this report, double ionization includes charge resonance enhanced ionization and short range double ionization. Amazingly, both double ionization paths contribute to the proton spectrum in Fig. 2 recorded without any group delay dispersion compensation. The peak at around 3 eV comes from charge resonance enhanced ionization while the higher-energy peak at 5.5 eV comes from short range double ionization. Group delay dispersion compensation is expected to be optimal at the interaction focal spot inside the ion spectrometer when the proton spectrum from H^++H^+ presents the highest energies. Indeed in this case, molecules interact with the shortest laser pulses, and the H_2^+ nuclear motion amplitude is expected to be reduced accordingly. More generally, this method is applied using Coulomb explosion of other molecules and looking for fragment energy shifts to higher energies as the pulse duration is reduced [12]. Group delayed dispersion compensation is tuned, inserting fused silica plates in the laser optical path. The best result is obtained with a 2-mm-thick fused

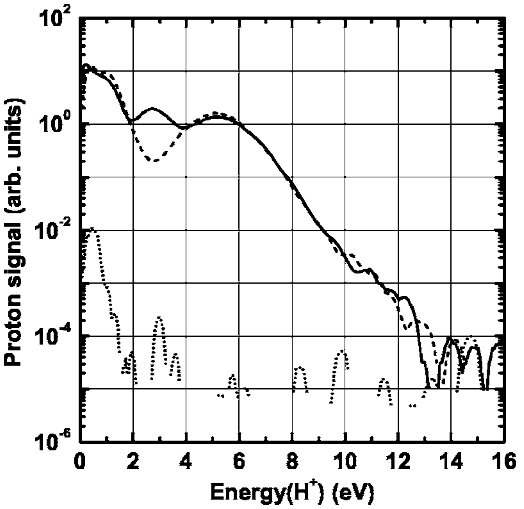

FIG. 3. Proton spectra recorded from H_2 using 10-fs pump, probe, and pump-probe laser excitation schemes. Dashed curve: pump pulse at 1.4×10^{15} W cm^{-2}. Dotted curve: probe pulse at 3.4×10^{13} W cm^{-2}. Full curve: the same above the pump and probe pulses, where the probe pulse delay is 24 fs.

silica plate after systematic trials with other plate thicknesses and variations of the number of reflexions on chirped mirrors placed after the Michelson interferometer. The corresponding proton spectrum is represented by the dotted curve in Fig. 2. The charge resonance enhanced ionization peak at ~3 eV is no more detected. The spectrum exhibits a pronounced dip between protons with energies below 3 eV coming from the dissociation of H_2^+ via $H^+ + H$ and protons with energies above 3 eV coming from the short range double ionization of H_2^+ and the subsequent fragmentation via $H^+ + H^+$. In the following, we will show that the charge resonance enhanced ionization peak comes from a laser post-pulse using a pump-probe excitation scheme.

From now on, the group delay dispersion is compensated using the 2-mm-thick fused silica plate for both the pump and probe pulses. Figure 3 presents three proton spectra for, respectively, pump, probe, and pump-probe excitation schemes. The pump proton spectra exhibits the same features as in Fig. 2. The probe pulse intensity is 3.4×10^{13} W cm^{-2}, a much lower intensity than the pump pulse in order to produce very few protons from the $H^+ + H^+$ dissociation channel. The corresponding spectrum only receives a noticeable contribution from low-energy protons below 2 eV coming from the $H^+ + H$ dissociation channel. The full curve represents the proton spectrum from the pump-probe excitation scheme using the same pulses as above and a probe delay of 24 fs. The charge resonance enhanced ionization peak at around 3 eV appears again. However, considering the single pulse excitation scheme of Fig. 2, this peak is now due to the delayed probe pulse. It is remarkable that the very high cross section of charge resonance enhanced ionization allows us to detect such a very weak post-pulse in comparison with the pump pulse. Considering proton spectra associated to the pump and probe pulses alone, this detection is only possible because of the noninstantaneous time response of charge resonance enhanced ionization that demands time delays larger than several femtoseconds between the first and second electron departures.

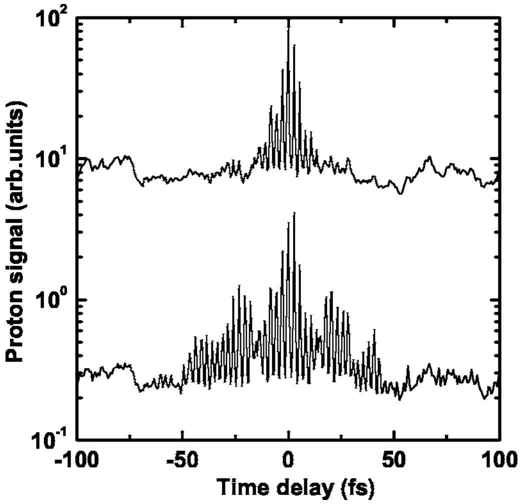

FIG. 4. Integrated proton signals from H_2 recorded with two identical 10-fs laser pulses as a function of the pulses delay. For each pulse, the peak laser intensity is 8.3×10^{13} W cm^{-2}. Lower curve: integrated proton signal from charge resonance enhanced ionization in the 2–4 eV energy range. Upper curve: integrated proton signal from short range double ionization in the 4–15 eV energy range.

Another way to show the sensitivity of proton spectra versus the presence of a post-pulse is to perform the equivalent of what is done with the interferometric autocorrelator. Two identical replicas of the initial 10-fs pulse are used to ionize the H_2 molecule and proton signals are recorded as a function of the pulses delay. In Fig. 4, the lower curve was recorded from protons coming from charge resonance enhanced ionization. The relative number of protons with energies from 2 to 4 eV is reported for each time delay. The upper curve corresponds to protons with energies from 4 to 15 eV coming from short range double ionization. The difference between the lower and upper curves is striking and comes basically from the different intensity dependent ionization yields of the H_2^+ ion, leading to the different $H^+ + H^+$ fragmentation channels. While the high-energy proton signal exhibits what is expected from a short few-cycle pulse, the low-energy proton signal from charge resonance enhanced ionization shows important wings around the main interference signal centered at zero delay. The sharp variations of the interferences are due to the 0.1-μm step of the interferometer delay line corresponding to a 0.67-fs temporal step. Charge-resonance enhanced ionization occurs at much lower laser intensities than short range double ionization. In consequence, when one of the pulse delayed by around 25-fs interferes with the wings of the other pulse, the intensity relatively weak increase is sufficient to produce low-energy protons while this is not the case for high-energy protons. Wings can be seen in Fig. 1 from the interferometric autocorrelation, but with a much lower contribution than in Fig. 4. Indeed, the second-order nonlinearity of the autocorrelator doubling crystal is weaker than the nonlinearity order of charge resonance enhanced ionization. This order is given by the tunnel ionization of H_2^+ since the subsequent ionization of H_2^+ is much more efficient. Following Ref. [10], the nonlinearity order of tunnel ionization of H_2 is ~6 for laser intensities well below the saturation intensity as in our case here in Fig. 4.

In conclusion, in this study it is shown that it is possible to separate in the time domain the ultrafast double ionization channels of H_2 coming, respectively, from charge resonance enhanced ionization and from short range double ionization. In particular, ultrashort 10-fs laser pulses allow us to isolate short range double ionization channels. Therefore charge resonance enhanced ionization is shown to be a good diagnostic for tuning group delay dispersion and detecting weak wings located at several tens of femtoseconds from the maximum of the laser pulse. Many techniques based on optoelectronics have been proven to be quite efficient for complete pulse characterization [15]. In this Rapid Communication we show that the double ionization of H_2 might become an efficient diagnostic of intense ultrashort laser pulses. However, the extraction of quantitative information demands a precise knowledge of the molecular response based on a nonperturbative time-dependent Schrödinger equation. Finally, let us emphasize here that short range double ionization includes several double ionization paths from sequential ionization to direct instantaneous two-electron emission with the important intermediate case of recollision that takes place within a fraction of the optical period [16,17]. The corresponding proton spectrum from 4 to 16 eV might be used as a sub-5-fs pulse diagnostic provided that ultrafast responses of the different paths are exactly known.

The authors are pleased to acknowledge the support of INTAS Grant No. 99-01495 and the support of ACI Photonique Physique Attoseconde.

---

[1] A. Giusti-Suzor, F. H. Mies, L. F. Di Mauro, E. Charron, and B. Yang, J. Phys. B **28**, 309 (1995).

[2] J. H. Posthumus, in *Molecules and Clusters in Intense Laser Fields* (Cambridge University Press, Cambridge, 2001).

[3] J. H. Posthumus, Rep. Prog. Phys. **67**, 623 (2004).

[4] P. H. Bucksbaum, A. Zavriyev, H. G. Muller, and D. W. Schumacher, Phys. Rev. Lett. **64**, 1883 (1990).

[5] T. Zuo and A. D. Bandrauk, Phys. Rev. A **52**, R2511 (1995).

[6] M. Nisoli, S. De Silvestri, and O. Svelto, Appl. Phys. Lett. **68**, 2793 (1996).

[7] S. Sartania, Z. Cheng, M. Lenzner, G. Tempea, C. Spielmann, F. Krausz, and K. Ferencz, Opt. Lett. **22**, 1562 (1997).

[8] H. Niikura, F. Légaré, R. Hasbani, M. Yu Yvanov, D. M. Villeneuve, and P. B. Corkum, Nature **421**, 826 (2003).

[9] X. Urbain, B. Fabre, V. M. Andrianarijaona, J. Jureta, J. H. Posthumus, A. Saenz, E. Baldit, and C. Cornaggia, Phys. Rev. Lett. **92**, 163004 (2004).

[10] G. N. Gibson, M. Li, C. Guo, and J. Neira, Phys. Rev. Lett. **79**, 2022 (1997).

[11] C. Trump, H. Rottke, M. Wittmann, G. Korn, W. Sandner, M. Lein, and V. Engel, Phys. Rev. A **62**, 063402 (2000).

[12] E. Baldit, S. Saugout, and C. Cornaggia, Phys. Rev. A **71**, 021403(R) (2005).

[13] W. C. Wiley and I. McLaren, Rev. Sci. Instrum. **26**, 1150 (1955).

[14] L. J. Frasinski, K. Codling, and P. A. Hatherly, Science **246**, 973 (1989).

[15] G. Steinmeyer, J. Opt. Soc. Am. A **5**, R1 (2003).

[16] K. J. Schafer, B. Yang, L. F. Di Mauro, and K. C. Kulander, Phys. Rev. Lett. **70**, 1599 (1993).

[17] P. B. Corkum, Phys. Rev. Lett. **71**, 1994 (1993).